Neurotherapeutics (2013) 10:340–353
DOI 10.1007/s13311-012-0168-z

ORIGINAL ARTICLE

A New Chiral Pyrrolyl α-Nitronyl Nitroxide Radical Attenuates β-Amyloid Deposition and Rescues Memory Deficits in a Mouse Model of Alzheimer Disease

Tian-yao Shi · Da-qing Zhao · Hai-bo Wang · Shufang Feng · Shui-bing Liu · Jiang-hao Xing · Yang Qu · Peng Gao · Xiao-li Sun · Ming-gao Zhao

Published online: 5 December 2012

Abstract The generation of reactive oxygen species causes cellular oxidative damage, and has been implicated in the etiology of Alzheimer's disease (AD). L-NNNBP, a new chiral pyrrolyl α-nitronyl nitroxide radical synthesized in our department, shows potential antioxidant effects. The purpose of this study was to investigate the protective effects of L-NNNBP on β-amyloid (Aβ) deposition and memory deficits in an AD model of APP/PS1 mice. In cultured cortical neurons, L-NNNBP acted as an antioxidant by quenching reactive oxygen species, inhibiting lipid peroxidation, nitrosative stress, and stimulating cellular antioxidant defenses. L-NNNBP inhibited cell apoptosis induced by Aβ exposure. *In vivo* treatment with L-NNNBP for 1 month induced a marked decrease in brain Aβ deposition and tau phosphorylation in the blinded study on APP/PS1 transgenic mice (1 mM in drinking water, initiated when the mice were 6 months old). The L-NNNBP-treated APP/PS1 mice showed decreased astrocyte activation and improved spatial learning and memory compared with the vehicle-treated APP/PS1 mice. These actions were more potent compared with that of curcumin, a natural product, and TEMPO, a nitroxide radical, which are used as free radical scavengers in clinics. These results proved that the newly synthesized L-NNNBP was an effective therapeutic agent for the prevention and treatment of AD.

Keywords Reactive oxygen species · Alzheimer disease · Nitroxide radical · L-NNNBP · β-amyloid

Introduction

Alzheimer's disease (AD), an age-related neurodegenerative disorder, is the most common form of dementia. AD is characterized by the deposition of β-amyloid (Aβ) plaques, intracellular neurofibrillary tangles, loss of neurons in the brain, progressive decline of memory and cognitive functions, and behavioral and personality changes [1–3]. In the pathogenesis and progression of AD, aging is the most critical risk factor. Moreover, oxidative stress has an important function in the early stages of AD [4, 5]. Reactive oxygen species (ROS)-mediated pathways are involved in AD development [6]. These findings have led to the development of neuroprotective strategies to prevent oxidative damage.

Several natural and synthetic compounds with potent antioxidant properties, such as spices, green tea, resveratrol, vitamins, Idebenone, and MitoQ, are therapeutic agents for AD [7, 8]. Curcumin is a major natural active component of the food flavoring turmeric (*Curcuma longa*); it has several times more potent antioxidation effects than vitamin E [9]. However, there is no difference between the curcumin-treated group

Tian-yao Shi, Da-qing Zhao, Hai-bo Wang and Shufang Feng contributed equally to this work.

T.-y. Shi · S.-b. Liu · J.-h. Xing · Y. Qu · M.-g. Zhao (✉)
Department of Pharmacology, School of Pharmacy, Fourth Military Medical University, Xi'an 710032, China
e-mail: minggao@fmmu.edu.cn

H.-b. Wang · P. Gao · X.-l. Sun
Department of Chemistry, School of Pharmacy, Fourth Military Medical University, Xi'an 710032, China

D.-q. Zhao
Department of Otolaryngology Head and Neck Surgery, School of Pharmacy, Fourth Military Medical University, Xi'an 710032, China

S. Feng
Department of Psychosomatics, Xijing Hospital, School of Pharmacy, Fourth Military Medical University, Xi'an 710032, China

and placebo group based on assessment of cognition, levels of isoprostanes, and Aβ levels [10]. MitoQ, a synthetic ubiquinone derivative, is a mitochondria-targeted antioxidant with a higher potential antioxidant effect. However, it did not show any improvement in patients with Parkinson's disease in a clinical trial [11]. For most antioxidant drugs, beneficial effects have been reported in cell cultures, and partially, in animal models. However, success in human clinical trials is much less frequent.

Nitroxide radicals (NRs) are stable free radicals stabilized by the delocalization of the unpaired electron over the N–O bond [12]. The TEMPO and α-nitronyl (NIT) groups are the two major kinds of NRs that have been most studied in the past two decades (Fig. 1A). Unlike other antioxidants that act in a sacrificial mode, NRs can provide protection in a catalytic manner (Fig. 1B). Through the continuous exchange between these forms NRs act as self-replenishing antioxidants that degrade superoxide and peroxide. Therefore, as a unique class of antioxidants, NRs have been exploited for many research and therapeutic applications, including protection against ionizing radiation [13], ischemia/reperfusion injury [14], and neurodegenerative diseases [15, 16]. Some applications of NRs have achieved good effects in clinical trials. For example, amifostine, a NR which is the first Food and Drugs Administration-approved radioprotective drug, is being used in clinical practice [17]. Tempol (4-hydroxy-2,2,6,6-tetramethylpiperidine-N-oxyl), a kind of TEMPO group NR, is found to be safe and well tolerated as a topical application to the scalp before brain radiation in a Phase I study. A Phase II study on tempol is underway [18].

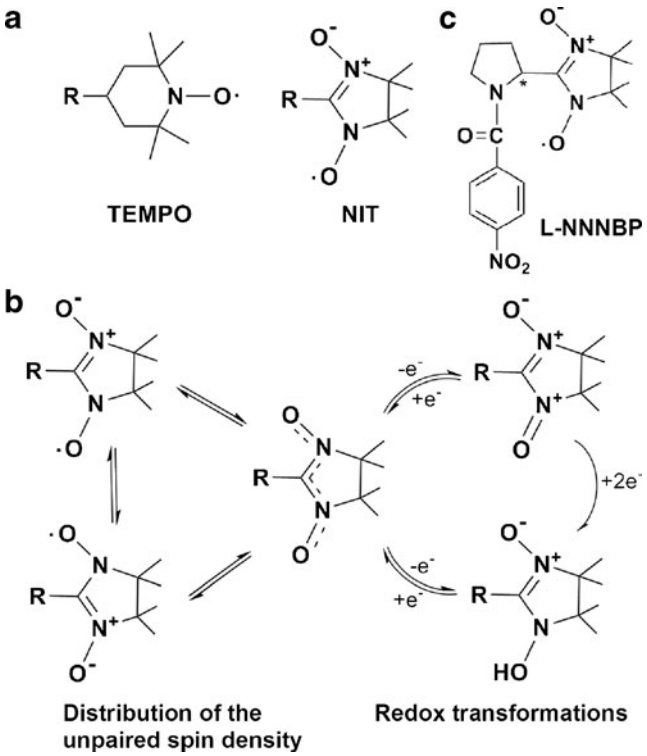

Fig. 1 Structure of L-NNNBP and other nitroxide radicals (NRs). (A) Structure of TEMPO and α-nitronyl (NIT). (B) NIT group NR structure exchanges between the forms. (C) Structure of L-NNNBP

Compared with the TEMPO group, NIT group NRs have an extensive distribution of unpaired spin density (Fig. 1A). Moreover, Rey [19] posited that the effects of the structural, magnetic, and optical properties, as well as the further biological effects of chiral NRs, can be changed after the introduction of the chiral center as close as possible to the oxyl group carrying most of the unpaired spin density. Thus, we synthesized a new chiral NR, L-N-p-nitrobenzoylpyrrolidinyl(4,5-dihydro-4,4,5,5-tetramethyl-3-oxido- 1H-imidazol-3-ium-1-oxyl-2-yl), (L-NNNBP, Fig. 1C) in our previous study.

In the present study we evaluated the effects of L-NNNBP on free radical scavenging *in vitro* and on neurodegenerative pathology and memory deficits in amyloid precursor protein (APP) and presenilin 1 (APP/PS1) double-transgenic mice, a well established AD mouse model [20]. Treatment with L-NNNBP for 4 weeks effectively reduced Aβ accumulation and tau hyperphosphorylation compared with the current free radical scavengers used in clinics, namely curcumin and tempol (TEMPO group achirality NRs).

Materials and Methods

Reagents

Cumine hydroperoxide (CHP), lucigenin, xanthine oxidase, and xanthine were purchased from Sigma Chemical Co. (St. Louis, MO). Thiobarbituric acid was obtained from Merck (Darmstadt). Other chemicals and reagents were from Sigma unless mentioned. All of the chemicals and reagents used were commercially available and of standard biochemical quality.

Superoxide Anion Radical-Scavenging Activity

Xanthine oxidase and xanthine-induced lucigenin chemiluminescence measurements were carried out as described previously [21]. The reaction mixture was composed of 100 μl of 100 μM xanthine, 50 μl of 800 μM lucigenin (both in a 50 mM sodium carbonate buffer at pH10.5), 25 μl of the drugs dissolved in distilled water, and 25 μl of 8 mU/ml xanthine oxidase in 2 M ammonium sulfate-containing 1 mM EDTA. The vehicle control contained only distilled water. The chemiluminescence (RLU/min) intensity was recorded for 10 min in a 96-well plate. The areas under the curve were calculated for comparison of drug effects.

Preparations of Liver Microsomes

Mouse liver microsomes were prepared by standard differential centrifugation techniques, as described by Satav and Katyare [22]. Briefly, mice were killed by ether anesthesia. The livers were removed quickly, washed with ice-cold saline, and weighed. One gram of liver tissue was homogenized with 4 ml of ice-cold 0.1 M Tris-HCl buffer (pH7.4) containing 0.25 M sucrose. The homogenate was centrifuged at 14,000×*g* for 30 min. The supernatant was collected and centrifuged at 165,000×*g* for 60 min. The resultant microsomes were washed with 0.1 M Tris-HCl buffer (pH 7.4) and stored at -80 °C. All procedures were carried out at 0–4 °C. The microsomes were suspended in 0.1 M Tris-HCl buffer (pH7.4) when used in the experiments. The Fourth Military Medical University Animal Care and Use Committee approved the animal protocols.

CHP-Induced Lipid Peroxidation

The microsomes (2 mg microsomal protein/ml) were pre-incubated with (I) or (I_0) in 0.1 M Tris–HCl buffer (pH7.4). Lipid peroxidation was initiated by CHP (1 mM) and the samples were incubated at 37 °C for 15 min. Trichloroacetic acid (10 %, w/v) was used to stop the reaction. The thiobarbituric acid reactive substances were determined as described [23]. The inhibitory effect on CHP-induced lipid peroxidation was calculated as follows: (%) inhibition ratio=$(I_0\text{-}I)/I_0\times100$. F2-isoprostanes (non-enzymatic oxidation of arachidonic acid) are considered as markers of oxidative stress [24]. F2-isoprostanes were determined with an immunoassay kit (Cayman, Ann Arbor, MI) according to the manufacturer's instructions [25].

Primary Cortical Neuronal Culture and $A\beta_{1\text{-}42}$ Treatment

The experiments were performed on C57BL/6 J mice (embryonic, 18-days-old of both genders). Cultured prefrontal cortex neurons were prepared as described previously [26]. Briefly, the prefrontal cortex was dissected, minced, and trypsinized for 15 min using 0.125 % trypsin (Invitrogen, Carlsbad, CA). The cells were seeded onto either 24-well plates containing glass coverslips (Fisher Scientific, Pittsburgh, PA), 100-mm dishes, or 96-well plates precoated with 50 μg/ml poly-D-lysine (Sigma) in water and grown in Neurobasal-A medium (Invitrogen) supplemented with B27 and 2 mM GlutaMax (Invitrogen). In the B27/Neurobasal medium, glial growth was reduced to <0.5 % of the nearly pure neuronal population, as assessed using immunocytochemistry for glial fibrillary acidic protein and neuron specific enolase [27]. The cultures were incubated at 37 °C in 95 % air/5 % carbon dioxide with 95 % humidity. The cultures were used for experiments on the 10th day *in vitro*. The cultures were incubated at 37 °C in 95 % air/5 % carbon dioxide with 95 % humidity. Cultures were used for experiments on the 10th day *in vitro*. Aliquots of $A\beta_{1\text{-}42}$ were prepared at a concentration of 1 mM in phosphate buffer saline (PBS; 0.1 M) and incubated for 5 days at 37 °C. On the test day, PBS was added to the solution to reach the final concentration. The neurons were rinsed briefly with PBS and then pretreated with 10 μM Curcumin, Tempol and L-NNNBP for 24 h, respectively, followed by exposure to 25 μM of $A\beta_{1\text{-}42}$ for 12 h in the same medium. Afterward, cells were washed 3 times and returned to the original culture medium for 24 h.

Cell Viability Assay

Cell viability was determined by cell counting kit-8 (CCK-8) to count living cells by combining WST-8 [2-(2-methoxy-4-nitrophenyl)-3-(4-nitrophenyl)-5-(2,4- disulfophenyl)-2H-tetrazolium] and 1-methoxy phenazine methosulfate [28]. Briefly, cells were seeded on a 96-well plate at a concentration of 10^5 cells per well. After treatment, 1 μM WT/GFX or dimethylsulfoxide for another 1 h and 10 μl of CCK-8 reagent was added and incubated for further 2 h. The absorbance was measured at 450 nm using a microplate reader. The data were obtained from 5 independent experiments.

Measurement of Apoptotic Cells by the Terminal Deoxynucleotidyl Transferase dUTP Nick End Labeling Assay

To identify apoptotic neurons, terminal deoxynucleotidyl transferase dUTP nick end labeling (TUNEL) assays using an *in situ* cell death detection kit (Roche Diagnostics, Mannheim) were performed according to the manufacturer's instructions, followed by counterstaining with 0.1 μg/ml 4′-6-diamidino-2-phenylindole. The number of TUNEL-positive cells was counted in 10 randomized fields under a fluorescent microscope.

Immunofluorescence Labeling

Cells on coverslips were fixed with 4 % paraformaldehyde for 20 min at room temperature. The cells were then rinsed in PBS, followed by incubation with primary rabbit monoclonal anti-cleaved caspase-3 (1:300; Cell Signaling Technology, Danvers, MA) and mouse monoclonal anti-Tuj (1:500, 1:500, Sigma), containing 1 % bovine serum albumin in PBS containing 0.1 % Triton X-100 (PBST) overnight at 4 °C. Cultures were then washed in PBS, incubated with Cy3 or fluorescein isothiocyanate-conjugated goat anti-rabbit/mouse IgG secondary antibodies in PBST containing 5 % goat serum for 1 h at 37 °C (1:200; nvitrogen).

Finally, the cultures were cover-slipped with antifade gel/mount aqueous mounting media (SouthernBiotech, Birmingham, AL) supplemented with 4′-6-diamidino-2-phenylindole nuclear dye (Sigma). All control cultures were incubated in PBS without primary antibodies.

Transgenic Mice and Drug Treatments

Male APP/PS1 double-transgenic mice used in this study were obtained from Model Animal Research Center of Nanjing University [strain name, B6C3-Tg (APPswe, PSEN1dE9)85Dbo/NJU]. These mice express a chimeric mouse/human APP containing the K595N/M596L Swedish mutations and a mutant human PS1 carrying the exon 9-deleted variant under the control of mouse prion promoter elements, directing transgene expression predominantly to central nervous system neurons [29]. Age- and gender-matched wild type littermates were used as controls for all experiments with APP/PS1 mutant mice. All animals were kept on a 12 h light/dark cycle, with a regular feeding and cage cleaning schedule. The animals were randomized for therapy trials and coded, and the operators and data analyzer remained double-blinded to which treatment they received until the code was broken at the completion of data collection. Male mice were treated with curcumin, tempol or L-NNNBP (1 mM in drinking water). The average daily drinking water of an adult mouse is 4–7 ml, and the molecular weight of L-NNNBP is 478.2. The LD50 of L-NNNBP in mice is 2128 mg/kg. Thus, the dose of L-NNNBP for mouse in present study was 55–100 mg/kg, which is about 5 % of the LD50. Treatment was started when the mice were 6 months old and was continued for 1 month. The use of 6-month-old APP/PS1 mice is based on previous reports demonstrating that these mice begin to have Aβ plaques as early as 2.5 months, and have a high Aβ load in hippocampal and cortical subareas from 6 months of age [20, 30]. The Fourth Military Medical University Animal Care and Use Committee approved the animal protocols.

Immunohistochemistry

After the behavioral studies, animals were anesthetized with an intraperitoneal injection of chloral hydrate (160 mg/kg) and perfused, first with PBS and then with 4 % paraformaldehyde in PBS. The brains were dehydrated in three steps of 2 h-long intervals in 70 %, 96 %, and 99 % ethanol solutions respectively. The brains were then left in xylene overnight before being embedded in paraffin. Paraffin blocks were sectioned horizontally with a microtome setting of 6 μm or 50 μm. The sections were floated in a warm water bath and mounted on SuperFrost-Plus (Menzel-Glazer, Braunschweig, Germany) glass slides. With a section interval of 12, 1 series of sections was collected in a systematic random manner from each animal. Each series contained 14–16 sections. Sections were kept overnight at 37 °C and then stored at room temperature until staining. Immunohistochemical procedures were performed using coronal sections as described above. Paraffin-embedded brain sections were deparaffined, rehydrated, and endogenous peroxidase quenched with hydrogen peroxide [1 % (v/v) in methanol], and microwaved for 5 min (with 650 W) in citrate buffer (10 mM sodium citrate, pH6). They were then incubated for 60 min in blocking buffer [10 % (v/v) goat normal serum (Bioscience Research Reagents, Temecula, CA) in PBS containing 0.1 % (v/v) Triton X-100 (Sigma)] and subsequently in appropriately diluted primary antibodies (overnight at 4 °C). After rinsing, the primary antibody was developed by incubating with cyanine3 (Cy3)-or fluorescein isothiocyanate-conjugated secondary antibodies against the corresponding species (1 h at room temperature) or by incubating with biotinylated secondary antibodies against the corresponding species (1 h at room temperature). This was followed by 3,3′-diaminobenzidine (DAB) (Vector Laboratories, Burlingame, CA), according to the instructions of the manufacturer for peroxidase labeling. The astrocytes were stained with a rabbit polyclonal glial fibrillary acidic protein (GFAP) antibody (Abcam, Cambridge, MA).

Histology and Quantification of Amyloid Deposition

The rat brain sections were stained with Congo red solution to identify the Aβ plaques. A commercially available Congo Red kit (Sigma) was used after the sections were counter-stained with Mayer's hematoxylin solution according to the manufacturer's protocol. Aβ plaques were detected using the Image-Pro Plus (Media Cybernetics, Silver Spring, MD) software to analyze the percentage area occupied by positive stain. Images with a field size of 600,000 μm^2 were collected using the 10× objective on an Olympus Optical microscope. One frontal cortical region and t3 hippocampal regions were analyzed to ensure that there was no regional bias in the hippocampal values.

Quantification of 3-Nitrotyrosine by Enzyme-Linked Immunosorbent Assay

The culture neurons and hippocampal tissues were normalized via bicinchoninic acid protein assay to generate homogenates. 3-Nitrotyrosine (3-NT) measurements were performed in the supernatants as described [31]. Samples and standards were incubated in microtiter wells coated with antibodies recognizing protein-bound and free 3-NT (Cell Sciences, Norwood, MA). Biotynilated second antibody, then streptavidine-peroxidase conjugate and tetramethylbenzidine were added to the wells. The enzyme reaction was stopped by addition of citric acid and the absorbance at 450 nm was measured using a plate reader (Molecular Devices, Sunnyvale, CA).

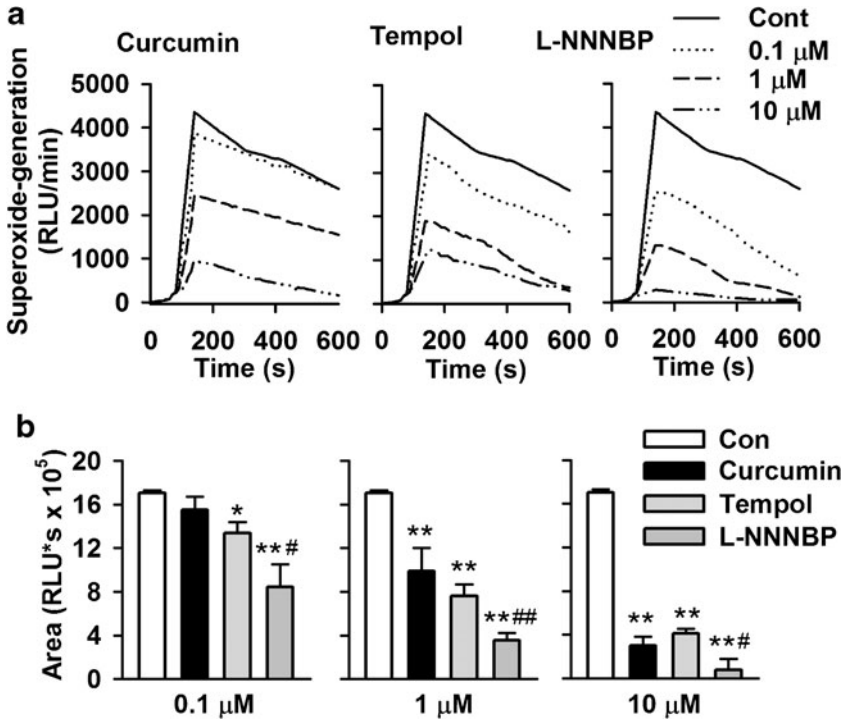

Fig. 2 Effects of L-NNNBP on superoxide generation. (A) L-NNNBP, curcumin or tempol blunted the chemiluminescence signals (RLU/min) in a dose-dependent manner. (B) The areas under the curve were evaluated. Columns show the mean integral values of chemiluminescence over 600 s. n=6 wells, *$P<0.05$, **$P<0.01$ compared with control; $^{\#}P<0.05$, $^{\#\#}P<0.01$ compared with curcumin and tempol treatments in the same concentration

Detection of Mitochondrial Membrane Potential

Mitochondrial membrane potential ($\Delta\psi_m$) in the culture neurons was detected as described previously [32]. The cationic fluorescent probe tetramethylrhodamine methyl ester (TMRM) accumulates in mitochondria because of the high membrane potential across the inner mitochondrial membrane. Neurons were incubated with $TMRM^+$ (20 nM) in experimental medium for 30 min, rinsed once with L-15, and viewed in L-15 containing 20 nM $TMRM^+$. At equilibrium, the fluorescence produced by $TMRM^+$ (excitation 543/emission red photomultiplier channel) is a direct function of $\Delta\psi_m$.

Western Blot Analysis

Western blot analysis was performed as described previously [26]. Equal amounts of protein (50 μg/lane) from the cultures were separated and electrotransferred onto polyvinylidene fluoride membranes (Invitrogen), which were incubated with rabbit polyclonal anti-tau (1:1000; Santa Cruz Biotechnology, Santa Cruz, CA), rabbit polyclonal anti-p-Tau (Ser235) (1:1000; Santa Cruz Biotechnology), rabbit polyclonal anti-p-Tau (Thr205) (1:1000; Santa Cruz Biotechnology), and mouse monoclonal anti-β-actin (1:4000; Sigma) as an internal control. The membranes were incubated with horseradish peroxidase-conjugated anti-rabbit or mouse IgG antibodies, and the bands were scanned with GS800 Densitometer Scanner (Bio-Rad, Hercules, CA) and optical density analyzed by Quantity One software (Bio-Rad).

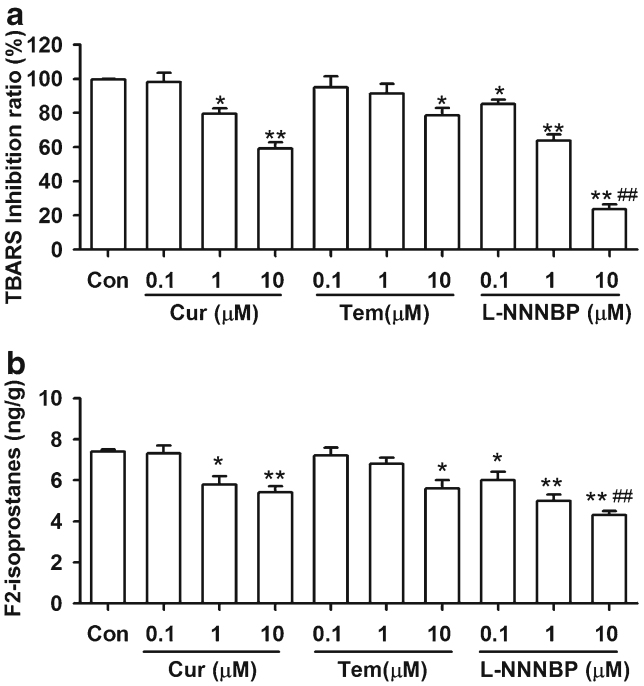

Fig. 3 Inhibition of lipid peroxidation by L-NNNBP. (A) The inhibitory rate of thiobarbituric acid reactive substances was compared between the curcumin (Cur), tempol (Tem), and L-NNNBP at three concentrations. (B) The levels of F2-isoprostanes were compared between curcumin, tempol, and L-NNNBP at three concentrations. n=6 wells from 3 independent experiments, *$P<0.05$, **$P<0.01$ compared with control; $^{\#}P<0.05$, $^{\#\#}P<0.01$ compared with curcumin and tempol treatments in the same concentration

Morris Water Maze Test

After treatment for 1 month, spatial learning and memory were evaluated by the Morris water maze test. The Morris water maze is a circular and galvanized water tank (120 cm diameter×50 cm height) filled to a depth of 25 cm with water. The surface area of the tank was divided into 4 equal quadrants. The water was made opaque by the addition of milk powder, and its temperature was adjusted to 24±1 °C. An escape platform (10 cm diameter) was placed in 1 of the 4 maze quadrants submerged 2 cm below the water surface (30 cm away from the side wall). The platform was kept at the same (target) quadrant during the entire course of the experiment. The mice were required to find the hidden platform using only distal spatial cues available in the testing room. Conditions were constant throughout the experiments. The mice were released gently into the water, always facing the tank wall. A different starting position was used on each trial. They were given 120 s to find the platform. On reaching the platform, the mice were allowed to remain on it for 10 s. They were taken out, dried, and placed in a separate cage for 60 min before the next trial. If a mouse failed to locate the platform within 120 s, it was assisted by the experimenter and allowed to stay there for the same period of time (10 s). Between the trials, the water was stirred to erase olfactory traces of previous swim patterns. The animals were trained for four trials per day for 5 consecutive days to locate and escape onto the platform, and their spatial learning scores (latency in seconds) were recorded. To assess memory consolidation, a probe trial was performed on days 8 and 9 after the 5 d acquisition tests. In this trial, the platform was removed from the tank, and the mice were allowed to swim freely. For these tests, time spent in the target quadrant within 90 s was recorded. The time spent in the target quadrant was taken to indicate the degree of memory consolidation that has taken place after learning. The time spent in the target quadrant was used as a measure of spatial memory. Behavior of the mice in the pool was recorded by a video camera positioned on the ceiling in the center of the testing room. The video camera was interfaced with the computerized video-tracking system (Shanghai Jiliang Software Technology Co., Shanghai), which permitted the off-line analysis of multiple behavioral parameters.

Statistical Analysis

The data were expressed as mean±SEM. Statistical comparisons were performed by analysis of variance (ANOVA). If the ANOVA was significant, *post hoc* comparisons were conducted using Tukey's test. In all cases, $p<0.05$ was considered statistically significant.

Results

Free Radical-Scavenging Activities of L-NNNBP

We first examined the ability of L-NNNBP to scavenge the superoxide anion radical. Lucigenin chemiluminescence

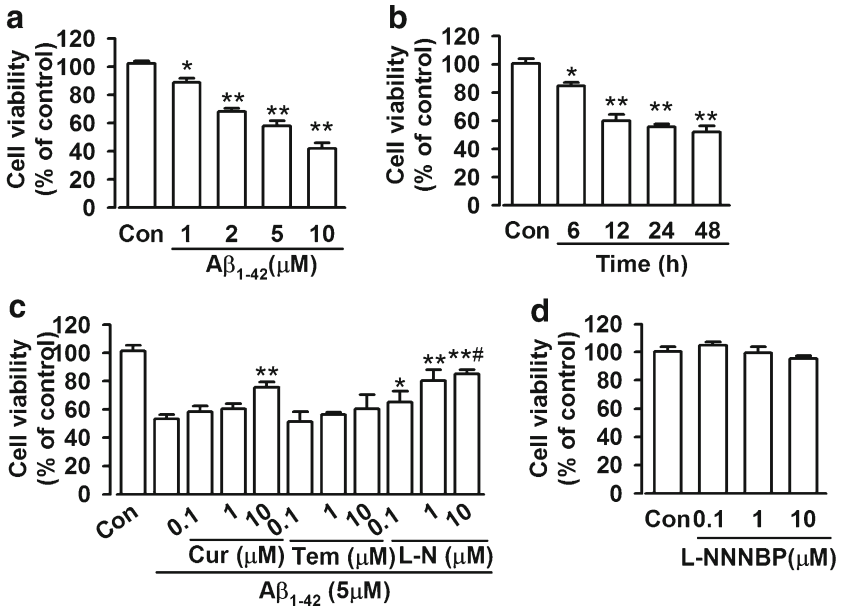

Fig. 4 Effects of L-NNNBP (L-N) on cell viability. (A) Dose-dependent cytotoxic effects of $A\beta_{1\text{-}42}$ on the cell viability of cortical neurons. *$P<0.05$, **$P<0.01$ compared with control. (B) Time-dependent cytotoxic effects of $A\beta_{1\text{-}42}$ on the cell viability of cortical neurons. *$P<0.05$, **$P<0.01$ compared with control. (C) Effects of curcumin (Cur), tempol (Tem) on the cell viability of cortical neurons after exposure to $A\beta_{1\text{-}42}$. *$P<0.05$ and **$P<0.01$ compared with $A\beta_{1\text{-}42}$ alone, $^{\#}P<0.05$ compared with curcumin+$A\beta_{1\text{-}42}$ or tempol+$A\beta_{1\text{-}42}$ in the same concentration. (D) L-NNNBP alone did not affect the cell viability. Values represent mean±SEM of 3 independent experiments

models derived from xanthine–xanthine oxidase reaction were also used to evaluate the free radical-scavenging activity of L-NNNBP. The areas under the curve were evaluated. As shown in Fig. 2A, the signals were quenched by adding curcumin, tempol or L-NNNBP in a dose-dependent manner. L-NNNBP showed more potent free-radical scavenging activities, which increased the chemiluminescence compared with curcumin and tempol at the same concentrations (Fig. 2B).

Inhibition of Lipid Peroxidation in Rat Liver Microsomes by L-NNNBP

In the CHP-induced lipid peroxidation system, the extent of thiobarbituric acid reactive substances formation was significantly decreased in the presence of L-NNNBP (Fig. 3A). L-NNNBP exhibited significant inhibition of lipid peroxidation, even at a concentration of 0.1 μM. Similarly, L-NNNBP inhibited the levels of F2-isoprostanes in a larger scale compared with the same concentrations of curcumin and tempol (Fig. 3B). Thus, L-NNNBP showed a higher inhibiting rate on lipid peroxidation compared with curcumin and tempol.

Neuroprotective Effects of L-NNNBP on $A\beta_{1-42}$-Induced Neurotoxicity

Cell viability was assessed via CCK-8 assays. Cell viability decreased upon $A\beta_{1-42}$ (1–10 μM) exposure in a concentration- and time-dependent manner (6–48 h) (Fig. 4A, B). Exposure to 5 μM $A\beta_{1-42}$ for 12 h resulted in approximately 60 % loss of cell viability, which was used in subsequent experiments. L-NNNBP, curcumin and tempol were pretreated 30 min before exposure to $A\beta_{1-42}$ and were co-existed with $A\beta_{1-42}$ for another 12 h. Then, the neurons were used for subsequent experiments. L-NNNBP attenuated $A\beta_{1-42}$-induced cell death in a concentration-dependent manner. However, tempol (0.1–10 μM) did not exhibit any neuroprotective activity against $A\beta_{1-42}$-induced toxicity (Fig. 4C). Curcumin exhibited neuroprotection only at a high concentration (10 μM); however, this neuroprotection was inferior to that mediated by L-NNNBP at the same concentration (Fig. 4C). Treatment with L-NNNBP alone did not affect the cell viability (Fig. 4D).

To distinguish further the features of apoptotic versus necrotic cells, TUNEL staining was performed to identify the apoptotic neurons. Neurons undergoing apoptosis were 59.2 %±7.3 % after $A\beta_{1-42}$ exposure for 12 h (Fig. 5A, B). Pretreatment of L-NNNBP (10 μM) significantly reduced apoptotic neurons to 22.7 %±2.6 %, and this anti-apoptotic activity was more significant than that mediated by the same concentrations of curcumin (42.9 %±3.1 %) and tempol (51.1 %±1.1 %) (Fig. 5B).

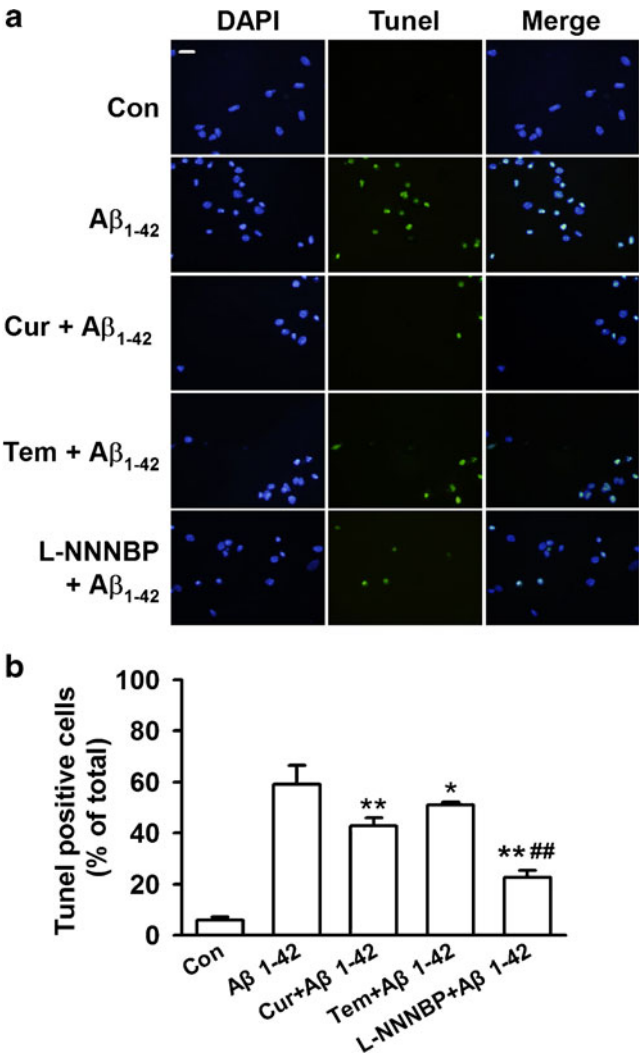

Fig. 5 Antiapoptotic activity by L-NNNBP. (A) Representative immunostaining and (B) quantitative assessment of apoptotic cell death by terminal deoxynucleotidyl transferase dUTP nick end labeling (TUNEL) assay. Fluorescent images (10× magnification): green, TUNEL; blue, 4′-6-diamidino-2-phenylindole (DAPI). Scale bar, 20 μm. $^{*}P<0.05$, $^{**}P<0.01$ compared with $A\beta_{1-42}$ alone; $^{\#\#}P<0.01$ compared with curcumin+$A\beta_{1-42}$ or tempol+$A\beta_{1-42}$. Values represent mean±SEM of 3 independent experiments, Cur=curcumin; Tem=tempol

L-NNNBP Treatment Reduced Active Caspase-3 Ratio

Procaspase-3 is an inactive form of cleaved caspase-3 and a major physiologic target of caspase-8 and caspase-9 [33]. Initiator caspase-8 directly activates procaspase-3 into active caspase-3, which causes Bcl-2 cleavage [34]. Thus, high active caspase-3 levels indicate high apoptotic activity. In this study, immunostaining indicated that $A\beta_{1-42}$ exposure induced a significant increase in cleaved caspase-3 expression (Fig. 6A). L-NNNBP (10 μM) notably reversed the cleaved caspase-3 levels and was more potent compared with curcumin or

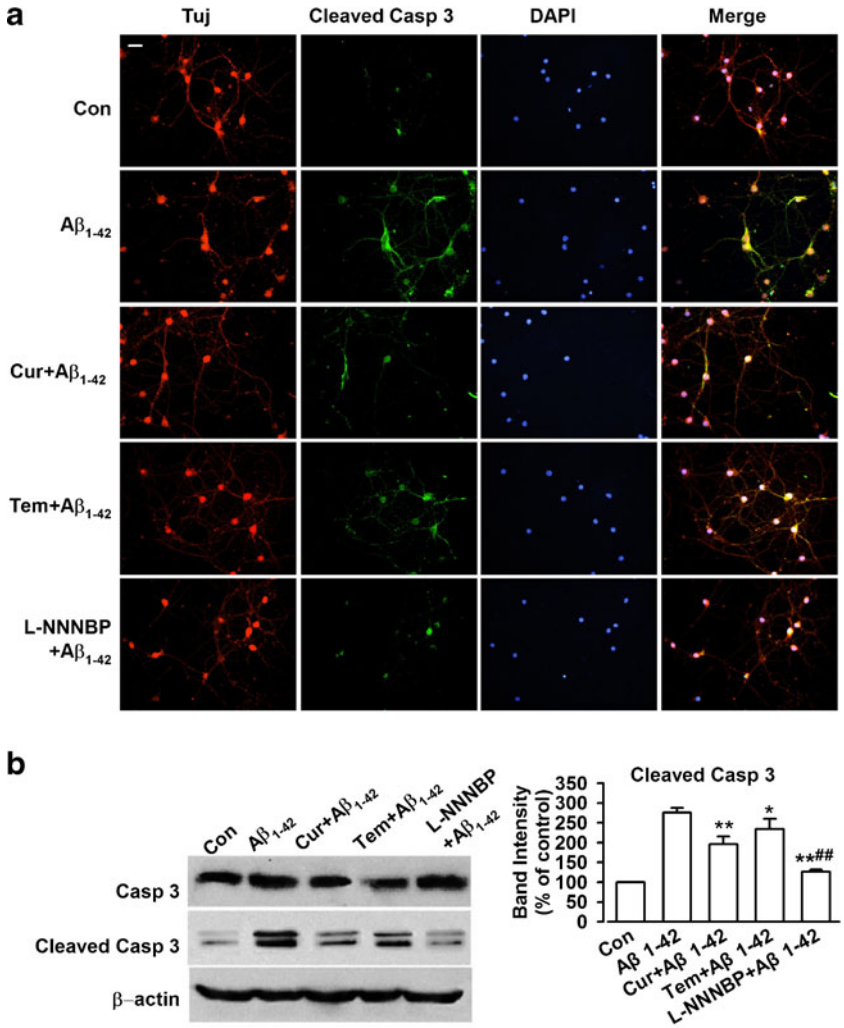

Fig. 6 Reduced active caspase-3 by L-NNNBP. (A) Representative immunostaining to show the expression of β-tubublin, cleaved caspase-3, and nuclei by the treatments. Scale bar, 20 μm. (B) Western blot results showing expression level of cleaved caspase-3. *$P<0.05$, **$P<0.01$ compared with $A\beta_{1\text{-}42}$ alone; $^{\#\#}P<0.01$ compared with curcumin (Cur) or tempol (Tem)+ $A\beta_{1\text{-}42}$. Data are expressed as mean±SEM of 3 independent experiments. DAPI=4′-6-diamidino-2-phenylindole

tempol at the same concentrations (Fig. 6A). Western blot analysis showed similar results to those obtained through the staining procedures performed in this study (Fig. 6B).

L-NNNBP Inhibits Nitrosative Stress and Mitochondrial Damage by $A\beta_{1\text{-}42}$ Exposure

We next examined the ability of L-NNNBP to inhibit nitrosative stress in the neurons with $A\beta_{1\text{-}42}$ exposure. 3-NT levels were increased in the neurons after $A\beta_{1\text{-}42}$ exposure for 12 h. L-NNNBP attenuated $A\beta_{1\text{-}42}$-induced 3-NT increase in a concentration- dependent manner. However, curcumin (10 μM) and tempol (0.1–10 μM) inhibited 3-NT levels only at higher concentrations (Fig. 7A). Furthermore, the inhibition of 3-NT by curcumin and tempol was weaker compared with that mediated by L-NNNBP at the same concentration (Fig. 7A).

Aβ exposure can cause mitochondrial dysfunction as evidenced by depolarization of mitochondrial membrane potential ($\Delta\psi_m$) [35]. $A\beta_{1\text{-}42}$ treatment for 12 h significantly depolarized Δψm, suggesting damage to the inner mitochondrial membrane. L-NNNBP (0.1–10 μM) prevented the depolarization of Δψm caused by $A\beta_{1\text{-}42}$ treatment, and this action was stronger that those of curcumin and tempol at the same concentration (Fig. 7B).

L-NNNBP Treatment Prevents Aβ Plaque Accumulation in APP/PS1 Mice

Curcumin decreased Aβ deposition in a transgenic AD mouse model [9], whereas tempol (1 mM in drinking water for 6 weeks) rescued the cerebrovascular function of APP transgenic mice [36]. Moreover, we detected the activities of L-NNNBP in the AD model of APP/PS1 mice. Treatments (1 mM in drinking water for 1 month) were started when the mice were 6 months old and were continued for 1 month. There was significant Aβ plaque accumulation in the hippocampus and sensory cortex of the APP/PS1 mice at 7 months. Treatment with L-NNNBP and tempol markedly reduced Aβ plaque accumulation in the hippocampus and

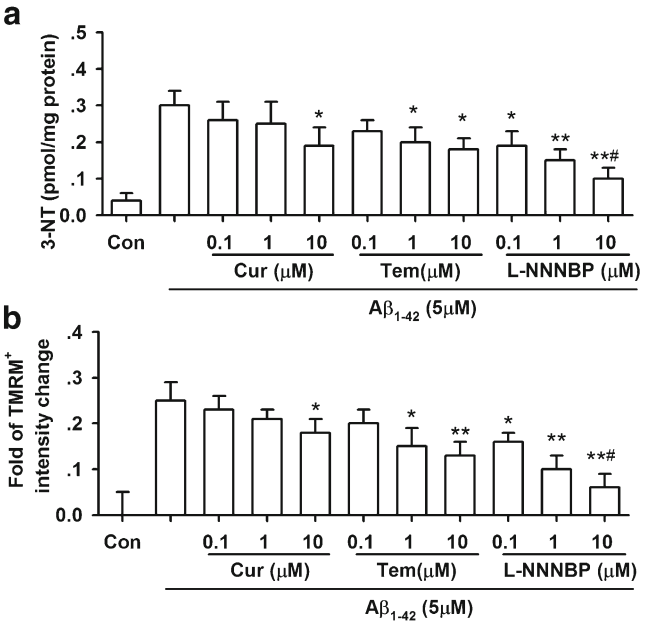

Fig. 7 Reduced nitrosative stress and mitochondrial damage by L-NNNBP. (A) Effects of curcumin, tempol, and L-NNNBP on the 3-nitrotyrosine levels of cortical neurons after exposure to $A\beta_{1\text{-}42}$. n=6 wells from 3 independent experiments, $^{*}P<0.05$ and $^{**}P<0.01$ compared with $A\beta_{1\text{-}42}$ alone, $^{\#}P<0.05$ compared with curcumin (Cur)+$A\beta_{1\text{-}42}$ or tempol (Tem)+$A\beta_{1\text{-}42}$ in the same concentration. (B) Effects of curcumin, tempol, and L-NNNBP on the depolarization of $\Delta\psi_m$ of cortical neurons after exposure to $A\beta_{1\text{-}42}$. n=6 wells from 3 independent experiments, $^{*}P<0.05$ and $^{**}P<0.01$ compared with $A\beta_{1\text{-}42}$ alone, $^{\#}P<0.05$ compared with curcumin+$A\beta_{1\text{-}42}$ or tempol+$A\beta_{1\text{-}42}$ in the same concentration

somatosensory cortex, whereas curcumin reduced Aβ plaque acumulation in the hippocampus only (Fig. 8A–C). Notably, treatment of L-NNNBP showed a higher ablity to prevent Aβ plaque accumulation (Fig. 8B, C) and lipid peroxidation, as shown by the levels of F2-isoprostanes in the brain (Fig. 8D) compared with curcumin or tempol.

L-NNNBP Prevents Tau Phosphorylation

Tau, a substrate for several protein kinases, is phosphorylated at over 38 serine/threonine residues in AD. Hyperphosphorylated tau appears in the APP/PS1 mouse brain after the onset of Aβ deposition [37]. Given the beneficial role of L-NNNBP in APP processing and Aβ deposition, we attempted to determine a possible role of L-NNNBP treatment in tau hyperphosphorylation in APP/PS1 mice. Tau hyperphosphorylation was assessed by Western blot using antibodies against the phosphorylation sites on Thr205 and Ser235. As shown in Fig. 9, enhancement of tau phosphorylation at Thr205 and Ser235 was observed in the hippocampus of the vehicle-treated APP/PS1 mice. By contrast, a marked decrease in Tau phosphorylation at Ser235 and Thr205 was observed in the L-NNNBP-treated APP/PS1 mice compared with the vehicle-treated mice (Fig. 9A). L-NNNBP markedly decreased tau phosphorylation compared with curcumin or tempol (Fig. 9B, C). No significant difference in the total Tau levels was noted between these groups (Fig. 9A).

We next examined the ability of L-NNNBP to inhibit nitrosative stress in the hippocampus of APP/PS1 mice. Higher levels of 3-NT were observed in the hippocampus of the vehicle-treated APP/PS1 mice compared with the wild type mice. A marked decrease in 3-NT levels was observed in the L-NNNBP-treated APP/PS1 mice compared with the vehicle-treated mice (Fig. 9D). However, curcumin treatment had no effect on the 3-NT levels in the APP/PS1 mice. Furthermore, the inhibition of 3-NT by L-NNNBP was more notable compared with that mediated by tempol at the same dosage (Fig. 9D).

L-NNNBP Treatment Inhibits Activation of Astrocytes in APP/PS1 Mice

In the brains of AD patients and transgenic AD mouse models, the infiltration of activated astrocytes are seen in the area of Aβ plaques [38, 39], which are characteristic components of an inflammatory process that develops around an injury in the brain. The activated astrocytes were visualized in brain sections stained with a GFAP antibody. A marked increase in reactive astrocytes was found in the somatosensory cortex of APP/PS1 mice compared with the wild type mice (Fig. 10A). The changes in the astrocytic reactivity were also confirmed by Western blot analysis (Fig. 10B). Treatment with L-NNNBP in APP/PS1 mice markedly inhibited the GFAP levels in the hippocampus. Quantitative analysis showed a 58.5 %±3.2 % decrease in GFAP expression in the L-NNNBP-treated APP/PS1 mice compared with that in the control APP/PS1 mice. The GFAP expression in the curcumin- or tempol-treated groups decreased by 17.6 %±2.8 % and 26.5 %±4.1 % , respectively, compared with the control APP/PS1 mice (Fig. 10B).

L-NNNBP Treatment Rescues Deficits of Learning and Memory in APP/PS1 Mice

The APP/PS1 AD mouse model develops Aβ-associated cognitive deterioration with increasing age [20]. Consistently, our study demonstrated that the vehicle-treated APP/PS1 mice showed impaired acquisition of spatial learning, as assessed by the Morris water maze test (Fig. 11A). These mice had impaired learning in using the available visuospatial cues to locate the submerged escape platform, as indicated by slower improvements in the escape latency across consecutive trials (Fig. 11B). The L-NNNBP-treated APP/PS1 mice reached the platform, which resulted in significantly reduced escape latency across the trials compared with the control APP/

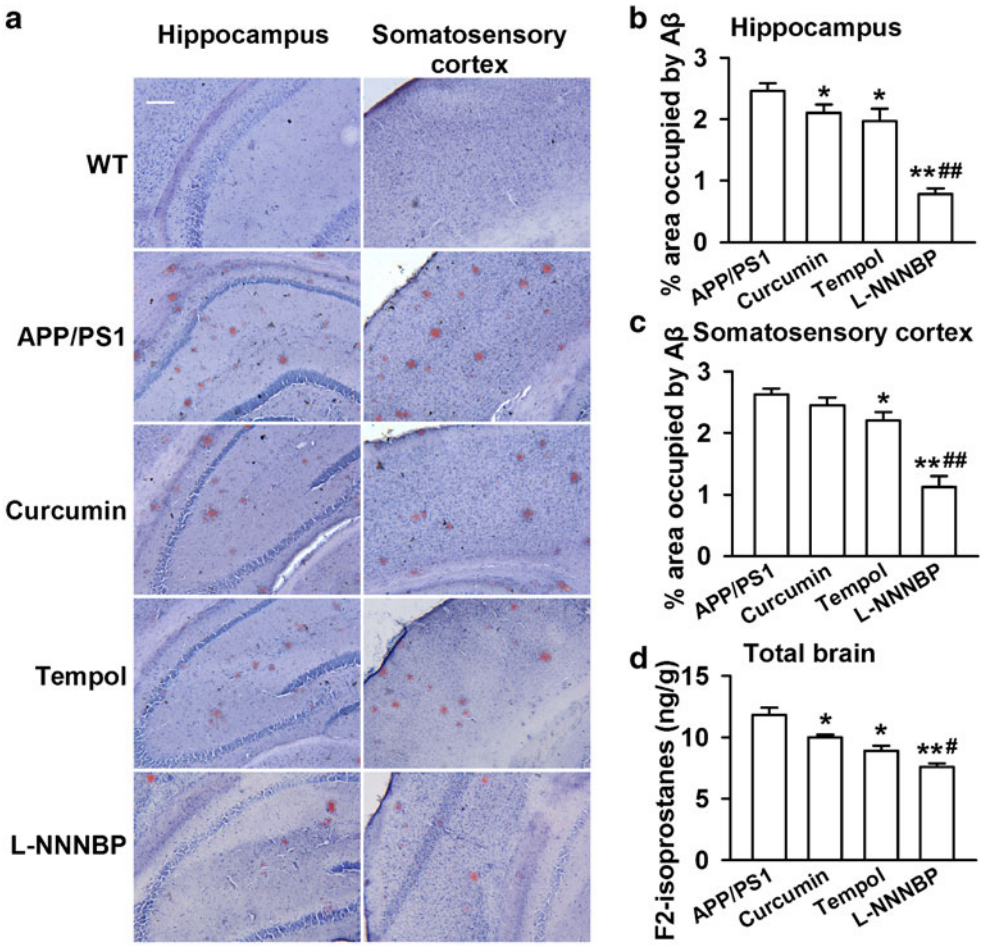

Fig. 8 Number of β-amyloid (Aβ) plaques in the brain. (A) Representative photomicrographs of brain Aβ plaques with Congo red staining in the hippocampus and somatosensory cortex regions of the 7-month-old transgenic mice. Scale bar, 100 μm. Histograms show the ratio of Aβ plaques in the hippocampus (B) and cortex (C) of the wild type (WT) and APP/PS1 mice. (D) The levels of F2-isoprostanes in the brain were compared between the curcumin, tempol, and L-NNNBP at 3 concentrations. The mice were sacrificed 1 day after the water maze test. n=5 mice in each group. *$P<0.05$, **$P<0.01$ compared with control APP/PS1 mice; $^{\#}P<0.05$, $^{\#\#}P<0.01$ compared with curcumin or tempol treatment in APP/PS1 mice

PS1 mice, and curcumin- and tempol-treated mice (Fig. 11B). Furthermore, we confirmed that L-NNNBP treatment significantly promoted learning during the hidden platform trials and significantly improved memory retention

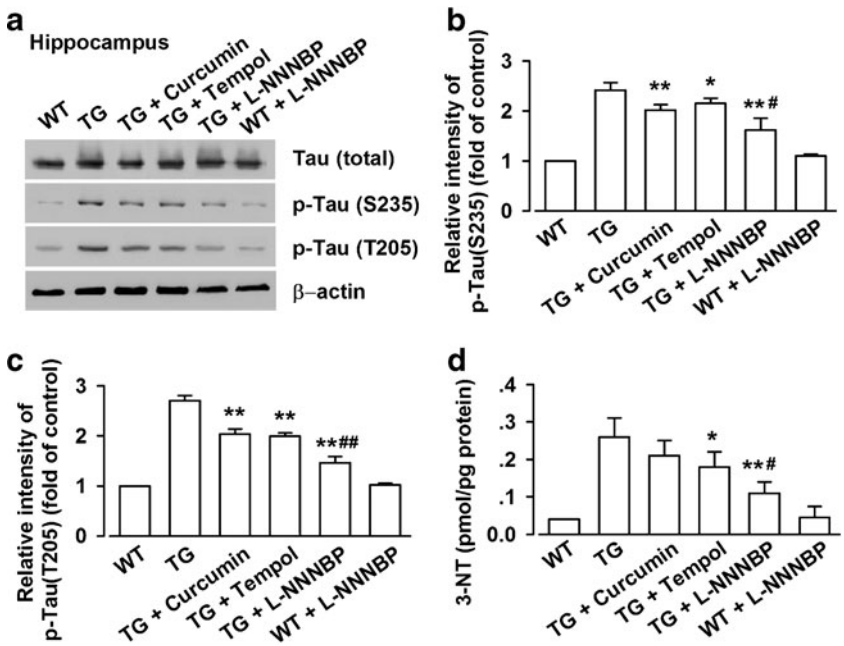

Fig. 9 L-NNNBP prevents tau phosphorylation. (A) Representative western blots of phosphorylated tau at Ser235, Thr205 and total tau expression in hippocampal lysates of wild type (WT) or APP/PS1 mice. (B) Quantitative analysis of phosphorylated tau at Ser235 expression. (C) Quantitative analysis of phosphorylated tau at Thr205 expression. (D) Effects of curcumin, tempol, and L-NNNBP on the 3-nitrotyrosine levels in hippocampal lysates of WT or APP/PS1 mice. n=6 mice in each group. *$P<0.05$, **$P<0.01$ compared with saline control APP/PS1 mice; $^{\#}P<0.05$, $^{\#}P<0.05$ compared with curcumin or tempol treatment in APP/PS1 mice. TG=transgenic mice

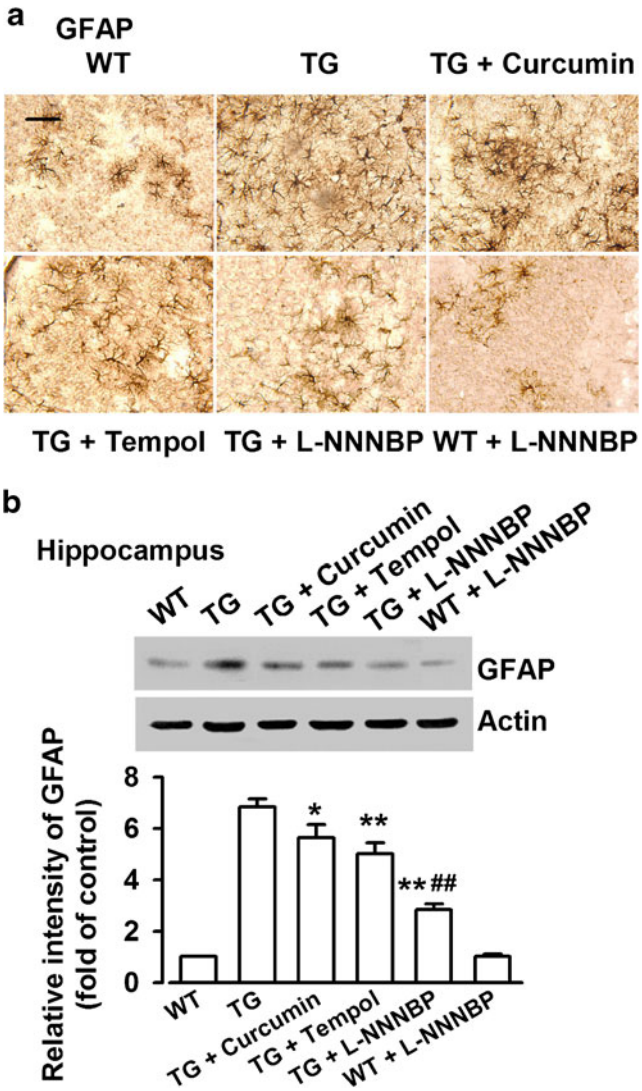

Fig. 10 Inhibition of astrocyte activation by L-NNNBP. (A) Staining of glial fibrillary acidic protein (GFAP) showing activated astrocytes in the somatosensory cortex. Scale bar, 20 μm. (B) Quantification of GFAP levels in wild type (WT) and APP/PS1 mice treated with vehicle or drugs (n=5 per group). *P<0.05, **P<0.01 compared with control APP/PS1 mice; $^{\#\#}P$<0.01 compared with curcumin or tempol in APP/PS1 mice. TG=transgenic mice

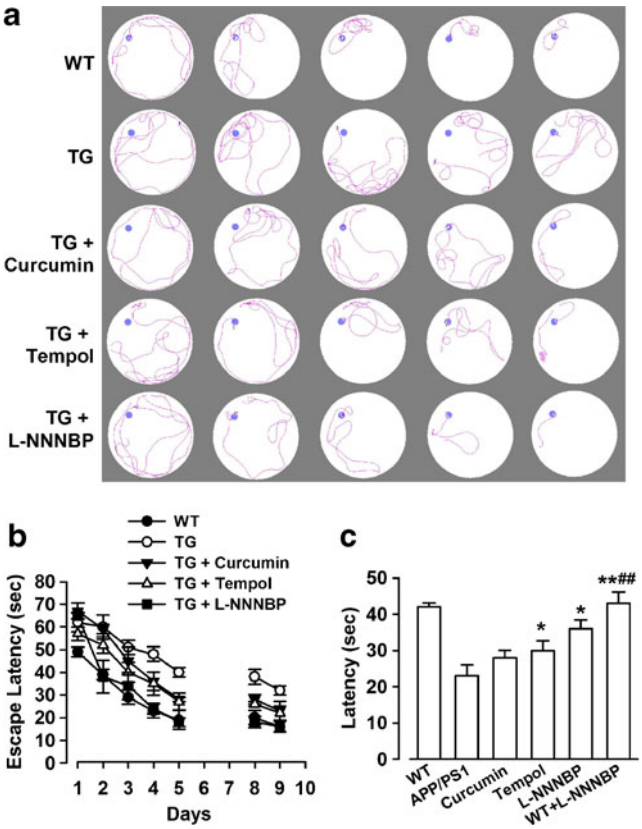

Fig. 11 Improvement of spatial memory by L-NNNBP. (A) Sample traces of acquisition of spatial learning in the Morris water maze hidden-platform task. (B) Latency score represents time taken to escape to the platform from the water. (C) Memory test in Morris water maze probe trial without platform. n=8 mice in each group. *P<0.05, **P<0.01 compared with control APP/PS1 mice; $^{\#\#}P$<0.01 compared with curcumin or tempol in APP/PS1 mice. TG=transgenic mice; WT=wild type

during the probe trial (Fig. 11C). L-NNNBP markedly improved the learning capability and memory of APP/PS1 mice compared with curcumin or tempol (Fig. 11B, C). L-NNNBP treatment did not affect the swimming ability of the APP/PS1 mice, as reflected by the similar swimming speeds between the groups (data not shown).

Discussion

Nitroxide radicals are utilized as biophysical tools in electronic spin resonance spectroscopic studies and spin-label oximetry. Oxidative stress has an important function in AD pathogenesis [6, 40, 41]. However, several strategies have been studied to prevent and/or slow down ROS-mediated damage. These strategies have beneficial effects in cell culture and, partially, in animal models, but with few successes in human clinical trials. One reason for this phenomenon may be that treatments are started very early in AD pathogenesis in animals, whereas in humans AD pathogenesis may be advanced by the time of diagnosis. Another reason may be the distribution or metabolism of antioxidants, which limits their ability to neutralize free radicals *in vivo*. Compared with other antioxidants, NRs have incomparable advantages of scavenging radicals through a rapid catalytic manner. The structure of NIT group NRs makes them priority antixidants among the NRs [42]. Combined with a chiral structure, the newly synthesized L-NNNBP shows stronger and faster antioxidant effects *in vitro* and *in vivo*.

Several free radical-generating models were used to evaluate the free radical-scavenging activity of L-NNNBP. Compared with other antioxidants, such as curcumin or tempol, L-NNNBP showed more notable free radical-scavenging activities at the same concentrations. The membrane lipids are particularly susceptible to oxidation owing to their high

concentration of polyunsaturated fatty acids and their association with the enzymatic and non-enzymatic systems in the cell membrane, which generate free radical species [43]. The antioxidants were tested for their antioxidant activities by measuring their abilities to inhibit CHP-induced lipid peroxidation in rat liver microsomes. The results of CHP-induced lipid peroxidation in rat liver microsomes also indicated that L-NNNBP exhibited a stronger antioxidant potential than curcumin or tempol did at the same concentrations.

$A\beta_{1\text{-}40}$ and $A\beta_{1\text{-}42}$ constitute the majority of Aβ found in human brain; they also participate in AD development and progression [44]. $A\beta_{1\text{-}42}$ is the more toxic of these species, both *in vitro* and *in vivo*. Some studies suggest that small Aβ oligomers are the actual toxic species of this peptide, rather than Aβ fibrils [45]. Formation of abnormal Aβ aggregates can lead to a series of complex pathogenic cascades that include disturbed cell signaling, mitochondrial dysfunction, and excitotoxicity [46]. Several of these pathogenic processes can produce free radical stress [47], which, in turn, can promote further Aβ aggregation, thereby potentially propagating pathogenic cascade from the reversible loss of synapses to neuronal death [48]. Using the cultured cortical neurons system, we demonstrated that pretreatment with L-NNNBP could significantly attenuate $A\beta_{1\text{-}42}$-induced cell viability loss. The L-NNNBP neuroprotection was partly owing to its antiapoptotic activities. In present study, the actions of L-NNNBP on TUNEL and caspase analysis are more obvious than that on the cell viability. The reason may be that apoptosis is the early event compared to cell death. Thus, the actions of L-NNNBP on the apoptotic proteins are more notable than the actions on the cell number quantification for the cell viability.

The activities of L-NNNBP were accessed in an Alzheimer's disease transgenic mouse model. There are many kinds of AD mutant mice. In general, oxidative damage is greater in mice with a single APP or PS1 mutation than in wild-type mice, and higher still in doubly transgenic mice expressing the combination of a mutant APP and mutant PS1 (APP/PS1) [49]. Therefore, using an APP/PS1 mouse model can better evaluate the effect of these antioxidant drugs. Curcumin decreased the levels of insoluble and soluble amyloid, and plaque burden by continuously feeding Tg2576 mice with a 160-ppm dose of curcumin for 6 months [9]. Tempol reduced Aβ plaque deposition and attenuated astroglial activation in APP mice after 6 weeks of treatment (1 mM in drinking water) [36]. In the present study, L-NNNBP treatment inhibited Aβ plaque accumulation and tau hyperphosphorylation in the APP/PS1 double-transgenic mice in as little as 4 weeks. This phenomenon led to the inhibition of astroglial activation, which is an important mediator in AD development [50], and in the improvement of spatial learning and memory.

Although the mechanism of Aβ plaque-induced neurotoxicity remains unclear, oxidative stress is a crucial factor in AD research [51]. $A\beta_{1\text{–}42}$ has a critical methionine residue at position 35. This Met35 residue is critical for $A\beta_{1\text{–}42}$ toxicity and oxidative stress [52]. The Met35 residue leads to the production of a sulfuranyl radical that can initiate free radical chain reactions with allylic H atoms on unsaturated acyl chains of lipids until a termination step is reached. Sulfuranyl radicals react with molecular oxygen to produce sulfoxide and superoxide [53]. Further, the sulfur-centered radical cation of Met35 gives rise to a hydrophobic environment that is ideal for lipid peroxidation in the lipid bilayer [54]. Therefore, antioxidation is an early and crucial step in the progression of $A\beta_{1\text{–}42}$-mediated lipid peroxidation. In our study, at the beginning of the appearance of the Aβ plaques, the APP/PS1 mice were treated continuously with L-NNNBP for 1 month. The findings indicate that L-NNNBP can prevent the Aβ deposition in a transgenic AD mouse.

NIT group NRs with more extensive distribution of the unpaired spin density are more suitable for structure modification. Introduction of chirality into NRs leads to structural diversity and uniqueness in their condensed phases owing to the relatively large electric dipole moment of the nitroxyl group and the magnetic moment arising from the unpaired electron [42]. When the chiral center is as close as possible to the oxyl group, which carries most of the unpaired spin, it can change the properties. L-NNNBP meets these requirements; it has a stable NIT group and a chiral center close to oxyl group. Therefore, L-NNNBP shows potent antioxidant actions probably owing to its special structure.

In conclusion, the newly synthesized L-NNNBP shows stronger and faster antioxidant effects *in vitro* and *in vivo* when the structure combines with a chiral structure. L-NNNBP acted as an antioxidant by quenching ROS, inhibiting lipid peroxidation, nitrosative stress, and stimulating cellular antioxidant defenses. These antioxidative activities of L-NNNBP are further proved by prevention of the neurotoxicity by $A\beta_{1\text{–}42}$ exposure and the memory deficit in the AD model of APP/PS1 transgenic mice. Aβ deposition and early cognitive impairment are preceded by mitochondrial dysfunction [55]. L-NNNBP prevented the depolarization of $\Delta\psi m$ caused by $A\beta_{1\text{-}42}$ treatment, suggesting that the beneficial activities of L-NNNBP are associated with prevention of the mitochondrial dysfunction. This study provides evidence that L-NNNBP, as a new chiral NR, is an effective candidate to prevent AD development. The free radical-scavenging property of potential nitroxide radicals makes the application of this kind of compound promising, although clinical trials on chiral NRs for AD prevention are not yet highly developed. The ultimate goals are to find a stronger ROS scavenger that is brain permeable and to develop a new kind of probe to be used in early diagnosis of AD.

Acknowledgments This research was supported by National Natural Science Foundation of China, No. 31070923, 31271144, 2011ZXJ09106-

01C, 2012BAK25B00, and 2011KTCL03-12. The authors state that no competing financial or other conflicts of interests exist.

Required Author Forms Disclosure forms provided by the authors are available with the online version of this article

References

1. Pratico D, Uryu K, Leight S, Trojanoswki JQ, Lee VM. Increased lipid peroxidation precedes amyloid plaque formation in an animal model of Alzheimer amyloidosis. J Neurosci 2001;21:4183-4187.
2. LaFerla FM, Green KN, Oddo S. Intracellular amyloid-beta in Alzheimer's disease. Nat Rev Neurosci 2007;8:499-509.
3. Reddy PH, Beal MF. Amyloid beta, mitochondrial dysfunction and synaptic damage: implications for cognitive decline in aging and Alzheimer's disease. Trends Mol Med 2008;14:45-53.
4. Nunomura A, Castellani RJ, Zhu X, Moreira PI, Perry G, Smith MA. Involvement of oxidative stress in Alzheimer disease. J Neuropathol Exp Neurol 2006;65:631-41.
5. Nunomura A, Perry G, Aliev G, et al. Oxidative damage is the earliest event in Alzheimer disease. J Neuropathol Exp Neurol 2001;60:759-767.
6. Lin MT, Beal MF. Mitochondrial dysfunction and oxidative stress in neurodegenerative diseases. Nature 2006;443:787-795.
7. Kim J, Lee HJ, Lee KW. Naturally occurring phytochemicals for the prevention of Alzheimer's disease. J Neurochem 2010;112:1415-1430.
8. Tauskela JS. MitoQ—a mitochondria-targeted antioxidant. IDrugs 2007;10:399-412.
9. Lim GP, Chu T, Yang F, Beech W, Frautschy SA, Cole GM. The curry spice curcumin reduces oxidative damage and amyloid pathology in an Alzheimer transgenic mouse. J Neurosci 2001;21:8370-8377.
10. Baum L, Lam CW, Cheung SK, et al. Six-month randomized, placebo-controlled, double-blind, pilot clinical trial of curcumin in patients with Alzheimer disease. J Clin Psychopharmacol 2008;28:110-113.
11. Snow BJ, Rolfe FL, Lockhart MM, et al. A double-blind, placebo-controlled study to assess the mitochondria-targeted antioxidant MitoQ as a disease-modifying therapy in Parkinson's disease. Mov Disord 2010;25:1670-1674.
12. Griller D, Ingold KU. Persistent carbon-centered radicals. Acc Chem Res 1976;9:13-19.
13. Hahn SM, Krishna MC, DeLuca AM, Coffin D, Mitchell JB. Evaluation of the hydroxylamine Tempol-H as an *in vivo* radioprotector. Free Radic Biol Med 2000;28:953-958.
14. Gelvan D, Saltman P, Powell SR. Cardiac reperfusion damage prevented by a nitroxide free radical. Proc Natl Acad Sci U S A 1991;88:4680-4684.
15. Dikalov SI, Vitek MP, Maples KR, Mason RP. Amyloid beta peptides do not form peptide-derived free radicals spontaneously, but can enhance metal-catalyzed oxidation of hydroxylamines to nitroxides. J Biol Chem 1999;274:9392-9399.
16. Liang Q, Smith AD, Pan S, et al. Neuroprotective effects of TEMPOL in central and peripheral nervous system models of Parkinson's disease. Biochem Pharmacol 2005;70:1371-1381.
17. Kouvaris JR, Kouloulias VE, Vlahos LJ. Amifostine: the first selective-target and broad-spectrum radioprotector. Oncologist 2007;12:738-747.
18. Metz JM, Smith D, Mick R, et al. A phase I study of topical Tempol for the prevention of alopecia induced by whole brain radiotherapy. Clin Cancer Res 2004;10:6411-6417.
19. Hirel C, Pécaut J, Choua S, et al. Enantiopure and racemic chiral nitronyl nitroxide free radicals: synthesis and characterization. Eur J Org Chem 2005;2005:348-359.
20. Trinchese F, Liu S, Battaglia F, Walter S, Mathews PM, Arancio O. Progressive age-related development of Alzheimer-like pathology in APP/PS1 mice. Ann Neurol 2004;55:801-814.
21. Galle J, Bengen J, Schollmeyer P, Wanner C. Impairment of endothelium-dependent dilation in rabbit renal arteries by oxidized lipoprotein(a). Role of oxygen-derived radicals. Circulation 1995;92:1582-1589.
22. Satav JG, Katyare SS. Effect of experimental thyrotoxicosis on oxidative phosphorylation in rat liver, kidney and brain mitochondria. Mol Cell Endocrinol 1982;28:173-189.
23. Xi M, Hai C, Tang H, Chen M, Fang K, Liang X. Antioxidant and antiglycation properties of total saponins extracted from traditional Chinese medicine used to treat diabetes mellitus. Phytother Res 2008;22:228-237.
24. Musiek ES, Morrow JD. F(2)-isoprostanes as markers of oxidant stress: an overview. Curr Protoc Toxicol 2005;Chapter 17:Unit17.5.
25. Shanu A, Groebler L, Kim HB, et al. Selenium inhibits renal oxidation and inflammation but not acute kidney injury in an animal model of rhabdomyolysis. Antioxid Redox Signal 2012 Oct 16 [Epub ahead of print].
26. Liu SB, Zhang N, Guo YY, et al. G-protein-coupled receptor 30 mediates rapid neuroprotective effects of estrogen via depression of NR2B-containing NMDA receptors. J Neurosci 2012;32:4887-4900.
27. Brewer GJ, Torricelli JR, Evege EK, Price PJ. Optimized survival of hippocampal neurons in B27-supplemented Neurobasal, a new serum-free medium combination. J Neurosci Res 1993;35:567-576.
28. Morita Y, Naka T, Kawazoe Y, et al. Signals transducers and activators of transcription (STAT)-induced STAT inhibitor-1 (SSI-1)/suppressor of cytokine signaling-1 (SOCS-1) suppresses tumor necrosis factor alpha-induced cell death in fibroblasts. Proc Natl Acad Sci U S A 2000;97:5405-5410.
29. Jankowsky JL, Fadale DJ, Anderson J, et al. Mutant presenilins specifically elevate the levels of the 42 residue beta-amyloid peptide *in vivo*: evidence for augmentation of a 42-specific gamma secretase. Hum Mol Genet 2004;13:159-170.
30. Blanchard V, Moussaoui S, Czech C, et al. Time sequence of maturation of dystrophic neurites associated with Abeta deposits in APP/PS1 transgenic mice. Exp Neurol 2003;184:247-263.
31. Bayir H, Kagan VE, Borisenko GG, et al. Enhanced oxidative stress in iNOS-deficient mice after traumatic brain injury: support for a neuroprotective role of iNOS. J Cereb Blood Flow Metab 2005;25:673-684.
32. McManus MJ, Murphy MP, Franklin JL. The mitochondria-targeted antioxidant MitoQ prevents loss of spatial memory retention and early neuropathology in a transgenic mouse model of Alzheimer's disease. J Neurosci 2011;31:15703-15715.
33. Stennicke HR, Jurgensmeier JM, Shin H, et al. Pro-caspase-3 is a major physiologic target of caspase-8. J Biol Chem 1998;273:27084-27090.
34. Kirsch DG, Doseff A, Chau BN, et al. Caspase-3-dependent cleavage of Bcl-2 promotes release of cytochrome c. J Biol Chem 1999;274:21155-21161.
35. Lustbader JW, Cirilli M, Lin C, et al. ABAD directly links Abeta to mitochondrial toxicity in Alzheimer's disease. Science 2004;304:448-452.
36. Nicolakakis N, Aboulkassim T, Ongali B, et al. Complete rescue of cerebrovascular function in aged Alzheimer's disease transgenic mice by antioxidants and pioglitazone, a peroxisome proliferator-activated receptor gamma agonist. J Neurosci 2008;28:9287-9296.
37. Kurt MA, Davies DC, Kidd M, Duff K, Howlett DR. Hyperphosphorylated tau and paired helical filament-like structures in the brains of mice carrying mutant amyloid precursor protein and mutant presenilin-1 transgenes. Neurobiol Dis 2003;14:89-97.
38. Itagaki S, McGeer PL, Akiyama H, Zhu S, Selkoe D. Relationship of microglia and astrocytes to amyloid deposits of Alzheimer disease. J Neuroimmunol 1989;24:173-182.

39. Matsuoka Y, Picciano M, Malester B, et al. Inflammatory responses to amyloidosis in a transgenic mouse model of Alzheimer's disease. Am J Pathol 2001;158:1345-1354.
40. Perry VH, Nicoll JA, Holmes C. Microglia in neurodegenerative disease. Nat Rev Neurol 2010;6:193-201.
41. Smith MA, Zhu X, Tabaton M, et al. Increased iron and free radical generation in preclinical Alzheimer disease and mild cognitive impairment. J Alzheimers Dis 2010;19:363-372.
42. Likhtenshtein GI, Yamauchi J, Nakatsuji Si, Smirnov AI, Tamura R. Organic functional materials containing chiral nitroxide radical units. Nitroxides. Wiley-VCH Verlag GmbH & Co, Berlin, 2008.
43. Aruoma O. Free radicals, oxidative stress, and antioxidants in human health and disease. J Am Oil Chem Soc 1998;75:199-212.
44. Selkoe DJ. Alzheimer's disease: genes, proteins, and therapy. Physiol Rev 2001;81:741-766.
45. Drake J, Link CD, Butterfield DA. Oxidative stress precedes fibrillar deposition of Alzheimer's disease amyloid beta-peptide (1-42) in a transgenic *Caenorhabditis elegans* model. Neurobiol Aging 2003;24:415-420.
46. Selkoe DJ. Alzheimer disease: mechanistic understanding predicts novel therapies. Ann Intern Med 2004;140:627-638.
47. Hardy J, Selkoe DJ. The amyloid hypothesis of Alzheimer's disease: progress and problems on the road to therapeutics. Science 2002;297:353-356.
48. Selkoe DJ. Alzheimer's disease is a synaptic failure. Science 2002;298:789-791.
49. Mohmmad Abdul H, Wenk GL, Gramling M, Hauss-Wegrzyniak B, Butterfield DA. APP and PS-1 mutations induce brain oxidative stress independent of dietary cholesterol: implications for Alzheimer's disease. Neurosci Lett 2004;368:148-150.
50. Garwood CJ, Pooler AM, Atherton J, Hanger DP, Noble W. Astrocytes are important mediators of Abeta-induced neurotoxicity and tau phosphorylation in primary culture. Cell Death Dis 2011;2:e167.
51. Zhu X, Su B, Wang X, Smith MA, Perry G. Causes of oxidative stress in Alzheimer disease. Cell Mol Life Sci 2007;64:2202-2210.
52. Butterfield DA, Boyd-Kimball D. The critical role of methionine 35 in Alzheimer's amyloid beta-peptide (1-42)-induced oxidative stress and neurotoxicity. Biochim Biophys Acta 2005;1703:149-156.
53. Miller BL, Williams TD, Schöneich C. Mechanism of sulfoxide formation through reaction of sulfur radical cation complexes with superoxide or hydroxide ion in oxygenated aqueous solution. J Am Chem Soc 1996;118:11014-11025.
54. Kanski J, Aksenova M, Butterfield DA. The hydrophobic environment of Met35 of Alzheimer's Abeta(1-42) is important for the neurotoxic and oxidative properties of the peptide. Neurotox Res 2002;4:219-223.
55. Yao J, Irwin RW, Zhao L, Nilsen J, Hamilton RT, Brinton RD. Mitochondrial bioenergetic deficit precedes Alzheimer's pathology in female mouse model of Alzheimer's disease. Proc Natl Acad Sci U S A 2009;106:14670-14675.